

Effect of antiferromagnetic coupling at interfaces on magnetic properties of Gd/CoFeTaB multilayers

Ou Xiang¹, Chengyue Xiong², Hong-Guang Piao^{1*}, Yingde Zhang³, Liqing Pan¹

¹ *Research Institute for Magnetoelectronics & Weak Magnetic-field Detection, College of Science, China Three Gorges University, Yichang 443002, P.R. China*

² *Key Laboratory of Advanced Materials (MOE) and Beijing National Center for Electron Microscopy, School of Materials Science and Engineering, Tsinghua University, Beijing 100084, P. R. China*

³ *Baotou Research Institute of Rare Earths, Baotou 014030, P.R. China*

***E-mail:** hgpio@ctgu.edu.cn

In this work, a multilayer structure composed of Gd and CoFeTaB was prepared by magnetron sputtering, and the effect of annealing temperatures on magnetic properties of the multilayer structure are investigated. The existence of interfacial antiferromagnetic coupling in this system was proved by analysis of microstructure, magnetic characteristics, and magnetic resonance characteristics. The preparation of artificial multilayer antiferromagnetic structure with weak stray fields was demonstrated, which provides a shortcut for spintronics application.

Understanding and control the interface of magnetic heterojunction is very important to spintronic applications. The magnetic heterojunction device based on spin-transfer torque¹ or spin-orbit torque² are typical designs of spintronics application. However, due to the influence of stray field around ferromagnetic materials on adjacent devices, this is bound to limit the further integration of spintronic devices^{3,4}.

In recent years, it has been found that the quantized state and ultrafast spin dynamic behaviors in antiferromagnetic materials can be controlled by optical or electrical means^{4,5}. Moreover, there is an antiparallel arrangement between adjacent atomic magnetic moments in antiferromagnetic materials, which inevitably makes it not present macroscopic magnetism and not susceptible to interference from external magnetic fields⁶. Therefore, antiferromagnetic materials are expected to replace ferromagnetic materials as the next generation of high-integration spintronic materials. But the spin states and dynamic behaviors of antiferromagnetic materials are not only difficult to detect but also difficult to control generally⁴. The electrical control of magnetism is one of most promising driving methods for spintronics devices, but the control of antiferromagnetic materials still needs to consume a lot of energy to achieve at present, which has hindered its application^{7,8}.

The artificial antiferromagnetic structure combines the advantages of antiferromagnetic material and ferromagnetic material, such as weak macroscopic magnetism, easy detection and control of magnetization states, high magnetoresistance signals etc. Recently, artificial composited material of TMs and REs have attracted much attention⁹⁻¹⁴, due to this combination have abundant magnetic phase diagrams¹⁵⁻¹⁷. Gadolinium (Gd) as a RE metal, has magnetic properties of strong atomic magnetic moment and large room temperature magnetic entropy change, which is often used in the field of permanent magnet technology and magnetic refrigeration technology^{18,19}. Amorphous CoFeTaB alloy as a TM alloy, has a unique combination of optical, electrical and ferromagnetic properties in one single material²⁰. If two multifunctional materials are combined into one device, it will have important implications for the spintronic applications. In the RE/TM multilayer system, there is an antiferromagnetic coupling at the interface. Therefore, the Gd/CoFeTaB multilayer as a RE/TM heterojunction system can expect similar to Gd/Fe multilayer systems¹⁵⁻¹⁷, that there is the antiferromagnetic coupling at interface.

In this work, microstructure, magnetic characteristics, and magnetic resonance characteristics of the Gd/CoFeTaB multilayer system were investigated with changing the annealing temperature. In order to further explore the possibility of application of the Gd/CoFeTaB system, the interfacial magnetic coupling mechanisms was discussed in this system.

Based on the $\text{Co}_{15}\text{Fe}_{55}\text{Ta}_{15}\text{B}_{15}$ alloy target, the $\text{CoFeTaB}(2\text{nm})/[\text{Gd}(4.8\text{nm})/\text{CoFeTaB}(2\text{nm})]_7$ multilayer structures (see Fig.1(a)) with 3-nm buffer and 5-nm capping layers of Ta were prepared by Magnetron Sputtering System (SKY Technology Development, JGP-560B, China) on the n-Si<100> substrates with a natural $\text{SiO}_2(2\text{nm})$ layer at the room temperature with a background pressure below 1×10^{-4} Pa. Under the argon (Ar, 99.99%) atmosphere, the Ta, CoFeTaB, and Gd layers were deposited with 0.3Pa, 0.5Pa, and 0.89Pa working pressures, respectively. To remove all possible oxide and impurities on the surface of targets, all targets were pre-sputtered for 3-min before depositing the sample. After the sputtering deposition, the samples were annealed in the vacuum annealing furnace (East Changing Technologies, China) with the 4×10^{-5} Pa at 200 °C, 300 °C, and 400 °C. Here, the heating rate set to be 10 °C/min, annealing was performed at the target temperature for 2 hours, and then completed by natural cooling. The microstructural characteristics of all samples were analyzed by X-ray Diffraction (XRD, Rigaku Ultima IV, Japan) with a conventional Cu-K α radiation source and Transmission Electron Microscopy (TEM, JEOL2010F, Japan). The magnetic characteristics and ferromagnetic resonance (FMR) properties were observed by the multifunctional Physical Property Measurement System (PPMS-VersaLab, Quantum Design, America) with changing the temperature condition.

The Fig.1(a) shows the schematic diagram of Ta/CoFeTaB/[Gd/CoFeTaB]₇/Ta multilayer structures on the SiO_2/Si substrate The Fig. 1(b) shows the XRD pattern of multilayer structures annealed at different temperatures. A sharp crystalline peak originating from the Si<100> substrate and a broad amorphous peak originating from the multilayer structure can be clearly. In the broad peak region, the Gd(100) peak on the XRD patterns of unannealed and annealed samples at 300°C and 400°C are faintly visible, which means that the Gd is easy to crystallize but cannot form a significant peak due to the signal interference between Gd layers. The Fig. 1 (c) shows a TEM image of unannealed sample, where can be observed

that the unannealed sample has an obvious multilayer structure on the SiO₂/Si substrate. As illustrated in the inset of Fig. 1 (c), the amorphous state of CoFeTaB layer can be clearly observed in the unannealed sample, while the scattered local crystalline state can be observed in the Gd layer. The Fig. 1 (d) shows a TEM image of annealed sample at 400°C, it is found that the annealing did not affect the Gd(4.8nm)/CoFeTaB(2nm) multilayer structure. After annealing, it was observed that the CoFeTaB layers still remained amorphous state, although the crystallization of Gd layers is more obvious, which can be attributed to the difference in microstructural systems between Gd and CoFeTaB materials.

To study the effect of annealing temperature (T_a) on the temperature-dependent magnetization (M) of Gd/CoFeTaB multilayer structures, under the 100 Oe auxiliary field, MT curves were measured with the zero field cooling (ZFC) and field cooling (FC) processes in the temperature range of 65~350K, as shown in Fig.2(a). The MT curve profile of multilayer structures is different from that of the pure Gd²¹ or CoFeTaB²² materials, the M does not decrease monotonously with the increase of temperature, which means that there may be magnetic coupling between Gd and CoFeTaB layers. Especially on the MT curve of the sample annealed at 400°C (see orange symbol curves), it is observed that the M first decreases and then increases, and then decreases, with the rise of temperature. As a composite system composed of TM and RE, the Gd/CoFeTaB multilayer structures should have a compensation temperature (T_{comp})^{10,23}. On this MT curve, it can also be clearly observed that a so-called T_{comp} is around 98K, which means that the antiferromagnetic coupling between Gd and CoFeTaB layers will be changed with increasing the temperature¹⁵, as schematically shown in inset of Fig.2(a). When $T < T_{\text{comp}}$, the Gd magnetic moment dominates in multilayer structures under external magnetic field. When $T_{\text{comp}} < T < T_c$, the CoFeTaB magnetic moment dominates in multilayer structures. The Gd magnetic moment is more sensitive to temperature dependence than CoFeTaB, which has been confirmed by MT characteristics of the pure Gd²¹ and CoFeTaB²² materials. It is worth noting that, our Gd(4.8nm)/CoFeTaB(2nm) multilayer system is very similar to the Gd(5nm)/Fe(3.5nm) multilayers²⁴, the magnetic phase transition temperature of Gd in the interface region is much higher than that of Gd in the bulk-like region, leads to more rich interfaces in TM/Gd multilayer systems, such as TM/Gd and Gd_{interface}/Gd_{bulk} interfaces, as shown in inset of

Fig.2(c). It can be proved that the existence of Gd_{bulk} region by the no compensated M at $T_{\text{comp}} = 98\text{K}$, as the black triangle shown in the Fig.2(a). From the overall trend profile of all the MT curves, the other samples should be similar to case of the sample annealed at 400°C , if not limited by the test temperature range. However, with the increase of annealing temperature, the M of multilayer structures shows a trend of decreasing on the whole. In addition, it is observed that there is no obvious bifurcation between the FC and ZFC processes in all the curves, which can confirm that there is no spin glass state²⁵. In addition, it's worth noting that the composite Currie temperature (T_c) of the multilayer structures is overall decreased trend with the increase of annealing temperature, although there is a slight increase after annealing at 400°C . The composite T_c of all samples is lower than Gd ($T_c=293\text{K}$)²⁴ and CoFeTaB²² (T_c more than 583K) films, which means that magnetic properties of the multilayer composite structure are obviously different from the simple Gd and CoFeTaB film systems because of the Gd/CoFeTaB interfacial effects in the system.

In-plane hysteresis (MH) loops of unannealed and annealed samples are measured under 65K , 150K and 300K . As shown in Fig.2(b) and Fig.2(c), all the samples exhibits a ferromagnetism under 65K and 150K , and are almost close to a state of saturation magnetization (M_s) when the magnetic field (H) increases to 4 kOe , except for the sample annealed at 400°C . Here, the M of the sample annealed at 400°C does not easily reach saturation state under 150K , this means that there is a non-ferromagnetic phase in the system. Moreover, a bee-waist hysteresis loop is observed in MH loops of all samples, as shown in Fig.2(c) as well as in the inset of Fig.2(b), which also indicates that different magnetic phases coexist in the system^{26,27}. Remember MT curves in Fig.2(a), each curve is not very smooth, which also indicate that the system has undergone a complex phase transition during the temperature change process. In addition, it is noteworthy that M_s at 65K ($<T_{\text{comp}}$) and 150K ($>T_{\text{comp}}$) of the annealed sample at 400°C are almost same, as the orange curve shown in Fig.2(a), which means that there are two kinds of anti-ferromagnetic coupling magnetic moment competition in the multilayer system. As shown in Fig.2(d), the M_s of all the samples decreases significantly at 300K which is far less than that of single CoFeTaB film (248 emu/cm^3 , see inset of Fig.3(d)) and Gd bulk (2020 emu/cm^3)²⁴, and the ferromagnetism is also not obvious compared with the low temperature, because all the samples have been

in the macroscopic paramagnetic state or the macroscopic weak-magnetic state higher than each composite T_c (see Fig.2(a)). Generally, annealing will enhance the magnetic order of the magnetic system, but it is abnormal in our multilayer system. From the Fig.1, it can also be observed that the crystalline order degree of Gd layers is improved with the increase of annealing temperature. However, it is found that the macroscopic M_s at 4 kOe and the coercivity (H_c) show an increasing and decreasing trend on the whole respectively, with the increase of annealing temperature, although the M_s and the H_c of annealed sample at 400°C have a slight recovery, as shown in inset of Fig.2(d). This result is very similar to the Gd/Co multilayer system which belongs to the same system as Gd/Fe multilayer structures^{28,29}, there also is an antiferromagnetic coupling at the $Gd_{interface}/CoFeTaB$ interface. With the increase of annealing temperature, the mutual diffusion of elements at the $Gd_{interface}/CoFeTaB$ interface will promote, which inevitably leads to the increase of interface roughness and the decrease of macroscopic M_s ²⁹. The increase of the interface roughness will also cause the increase of the pinning center of the magnetic domain wall at the interface, which will increase the H_c ²⁸. However, the crystallization of Gd layer gradually impedes the mutual diffusion of elements at interface, which can inhibit the interface roughness caused by annealing, and be beneficial to the increase of macroscopic M_s as well as the decrease of H_c .

All the samples were analyzed by magnetic resonance (FMR) spectroscopy at 70K, 150K and 300K. The FMR microwave range was 2~10 GHz and the scanning magnetic field was 0~3kOe. However, In-plane FMR signals at 150K were detected in both unannealed and annealed samples, except for the sample annealed at 400°C, as shown in Fig.3(a). Moreover, no FMR signals were detected in all samples at 70K and 300K. From the Fig.3(a), it is found that the FMR signals gradually weaken as the annealing temperature increases.

The relationship between the resonance field (H_f) and the resonance frequency (f) was obtained from the FMR signals, as shown in the Fig.3(b). It is found that the results are in good agreement with Kittel's equation³⁰, $f = \gamma\mu_0/2\pi \cdot \sqrt{H_f(H_f + M_s)}$. Where, γ is a gyromagnetic ratio and μ_0 is a permeability of vacuum. It can be observed that the M_s of multilayer structures is decreased with the increase of annealing temperature (see the yellow arrow), which result was also observed in the hysteresis loop at 150K (see Fig.2(c)). The M_s at 150K of unannealed Gd/CoFeTaB multilayer structure is lower than that of single

unannealed CoFeTaB film, which means that there is the anti-ferromagnetic coupling at the Gd/CoFeTaB interface, as schematically shown in inset of Fig.2(a). Moreover, it is observed that the M_s of CoFeTaB films increases with the increase of annealing temperature (see inset of Fig.3(d)), but the M_s of our multilayer structures decreases with the increase of annealing temperature (see Fig.2(d)). This means that the reduction in macroscopic M_s of Gd/CoFeTaB multilayer structures caused by annealing is due to the magnetic compensation effect of Gd layers.

The relationship between f and ΔH (the full width at half maximum (FWHM) of FMR spectrum), $\Delta H = 4\pi\alpha f/\gamma + \Delta H_0$ ³¹, was obtained from the FMR signals, as shown in the Fig.3(e). Here, ΔH_0 is a frequency-independent factor attributed to inhomogeneous linewidth broadening which is typically attributed to variations in the intrinsic sample properties³². The Gilbert damping constant, α , can be calculated by the relationship between f and ΔH , such as $\alpha \approx 0.02$ for the single CoFeTaB film, $\alpha \approx 0.07$ for the unannealed Gd/CoFeTaB multilayer sample, and $\alpha \approx 0.10$ (0.11) for the multilayer sample annealed at 200°C (300°C). When CoFeTaB is in a single film, the α was small, but when it is combined with Gd to form a multilayer structure, the α increases by about 3.5 times at 150K. By the comparison of hysteresis loops of unannealed Gd/CoFeTaB multilayer sample (see Fig.2(d)) and single CoFeTaB sample (see inset of Fig.3(d)), although the M_s of the multilayer sample was reduced by about 82.3 % after the combination of Gd and CoFeTaB, but the α can still be significantly increased due to the magnetic susceptibility (χ) also decreased by about 99.8 %, according to $\alpha \propto M_s(1 + \chi^{-1})$ ³³. This effectively demonstrates the introduction of antiferromagnetic coupling at the interface when Gd and CoFeTaB are combined into a multilayer structure. In addition, it can be observed from the Fig.3(e) that the α of the multilayer sample further increases with the increase of annealing temperature, which is attributed to the increase of $Gd_{\text{interface}}$ thickness³⁴ caused by annealing leading to the enhancement of antiferromagnetic coupling at the Gd/CoFeTaB interface.

In summary, the existence of interfacial antiferromagnetic coupling is proved by studying the effect of annealing temperature on the magnetic properties of CoFeTaB/Gd multilayer structures. It is also demonstrated the feasibility of the artificial multilayer antiferromagnetic

structure composed of TM and RE, which provides the possibility for the realization of spintronics devices without stray field.

Acknowledgments

This work was supported by the National Key R&D Program of China (Grant Nos. 2017YFB0903700 and 2017YFB0903702), the Key Laboratory of Advanced Materials of Ministry of Education Open Project (Grant No. 53220330118), and the National Natural Science Foundation of China (Grant Nos. 11474183).

References

- ¹M. D. Stiles, and A. Zangwill, Phys. Rev. B 66, 014407 (2002).
- ²I. M. Mihai, K. Garello, G. Gaudin, P-J Zermatten, M V. Costache, S. Auffret, S. Bandiera, B. Rodmacq, A. Schuhl, and P. Gambardella, Nature 476,189 (2011).
- ³X. Martí, I. Fina, and T. Jungwirth, IEEE Trans. Magn. 51, 1 (2015).
- ⁴T. Jungwirth, X. Marti, P. Wadley, and J. Wunderlich., Nat. Nanotechnol. 3, 231 (2016)
- ⁵X. Chen, X. Zhou, R. Chen, C. Song, J. Zhang, Y. Wu, Y. Ba, H. Li, Y. Sun, Y. You, Y. Zhao, and F. Pan, Nat. Mater. 18, 931 (2019).
- ⁶X. Marti, I. Fina, C. Frontera, J. Liu, P. Wadley, Q. He, R. J. Paull, J. D. Clarkson, J. Kudrnovský, I. Turek, J. Kuneš, D. Yi, J.-H. Chu, C. T. Nelson, L. You, E. Arenholz, S. Salahuddin, J. Fontcuberta, T. Jungwirth, and R. Ramesh , Nat. Mater. 13, 367 (2014).
- ⁷P. Wadley B. Howells, J. Železný, C. Andrews, V. Hills, R. P. Campion, V. Novák, K. Olejník, F. Maccherozzi, S. S. Dhesi, S. Y. Martin, T. Wagner, J. Wunderlich, F. Freimuth, Y. Mokrousov, J. Kuneš, J. S. Chauhan, M. J. Grzybowski, A. W. Rushforth, K. W. Edmonds, B. L. Gallagher, and T. Jungwirth , Science, 351, 587 (2016)
- ⁸S. Yu. Bodnar, *et al.*, Nat. Commun. 9, 348 (2018).
- ⁹L. Mouketo, N. Binggeli, and B. M'Passi-Mabiala, J Phys.: Condes. Matter 22, 186003 (2010).
- ¹⁰J. P. Andrés, L. Chico, J. Colino, and J. M. Riveiro., Phys. Rev. B 66, 094424 (2002).
- ¹¹P. N. Lapa, J. Ding, J. E. Pearson, V. Novosad, J, S. Jiang, and A. Hoffmann, Phys. Rev. B 96, 024418 (2017).
- ¹²A. B. Drovosekov, N. M. Kreines, A. O. Savitsky, E. A. Kravtsov, M. V. Ryabukhina, V. V. Proglyado, and V. V. Ustinov, J Phys.: Condes. Matter 29, 115802 (2017).

- ¹³A. Pogorily, E. Shypil, and C. Alexander, *J. Magn. Magn. Mater.* 286, 493 (2005).
- ¹⁴T. Seki, A. Miura, K. Uchida, T. Kubota, and K. Takanashi, *Appl. Phys. Exp.* 12, 023006 (2019).
- ¹⁵R. E. Camley, and D. R. Tilley, *Phys. Rev. B* 37, 3413 (1988).
- ¹⁶M. Sajieddine, Ph. Bauer, K. Cherifi, C. Dufour, and G. Marchal, *Phys. Rev. B* 49, 8815 (1994).
- ¹⁷W. Hahn, M. Loewenhaupt, Y. Y. Huang, G. P. Felcher, and S. S. P. Parkin, *Phys. Rev. B* 52, 16041 (1995).
- ¹⁸A. O. Pecharsky, K. A. Gschneidner, and V. K. Pecharsky, *J. Appl. Phys.* 93, 4722 (2003).
- ¹⁹C. L. Zhang, D. H. Wang, Z. D. Han, H. C. Xuan, B. X. Gu, and Y. W. Du, *J. Appl. Phys.* 105, 013912 (2009).
- ²⁰W. Liu, H. Zhang, J. Shi, Z. Wang, C. Song, X. Wang, S. Lu, X. Zhou, L. Gu, D. V. Louzguine-Luzgin, M. Chen, K. Yao, and N. Chen, *Nat. Commun.* 7, 13497 (2017).
- ²¹S. V. Taskaev, M. D. Kuz'min, K. P. Skokov, D. Yu. Karpenkov, A. P. Pellenen, V. D. Buchelnilov, and O. Gutfleisch, *J. Magn. Magn. Mater.* 331, 33 (2013).
- ²²Y. Zhang, S. Zhao, C Song, W. Liu, K. Yao, and N. Chen, *Mater. Des.* 143, 65 (2018).
- ²³S. Demirtas, and A. R. Koymen, *J. Appl. Phys.* 95, 4949 (2004).
- ²⁴D. Haskel, G. Srajer, J. C. Lang, J. Pollmann, C. S. Nelson, J. S. Jiang, and S. D. Bader, *Phys. Rev. Lett.* 87, 207201 (2001).
- ²⁵H. Hiroyoshi, and K. Fukamichi, *J. Appl. Phys.* 53, 2226 (1982).
- ²⁶E. Popova, N. Keller, F. Jomard, L. Thomas, M.-C. Brianso, F. Gendron, M. Guyot, and M. Tessier, *Eur. Phys. J. B* 31, 69 (2003).
- ²⁷L. H. Bennett, and E. D. Torre, *J. Appl. Phys.* 97, 10E502 (2005).

²⁸S. Vorobiov, Ia. Lytvynenko, T. Haute, M. Hehn, D. Derecha, and A. Chornous, *Vacuum*. 120, 9 (2015).

²⁹M. A. Basha, C. L. Prajapat, M. Gupta, H. Bhatt, Y. Kumar, S. K. Ghosh, V. Karki, S. Basu, and S. Singh, *Phys. Chem. Chem. Phys.* 20, 21580 (2018).

³⁰C. Kittel, *Phys. Rev.* 73, 155 (1948).

³¹S. S. Kalarickal, P. Krivosik, M. Wu, C. E. Patton, M. L. Schneider, P. Kabos, T. J. Silva, and J. P. Nibarger, *J. Appl. Phys.* 99, 093909 (2006).

³²A. Houshang, M. Fazlali, S. R. Sani, P. Dürrenfeld, E. Iacocca, J. Åkerman, and R. K. Dumas, *IEEE. Magn. Lett.* 5, 1 (2014).

³³M. C. Hickey, and J. S. Moodera, *Phys. Rev. Lett.* 102, 137601 (2009).

³⁴R. Bansal, N. Chowdhury, and P. K. Muduli, *Appl. Phys. Lett.* 112, 262403 (2018).

Figures

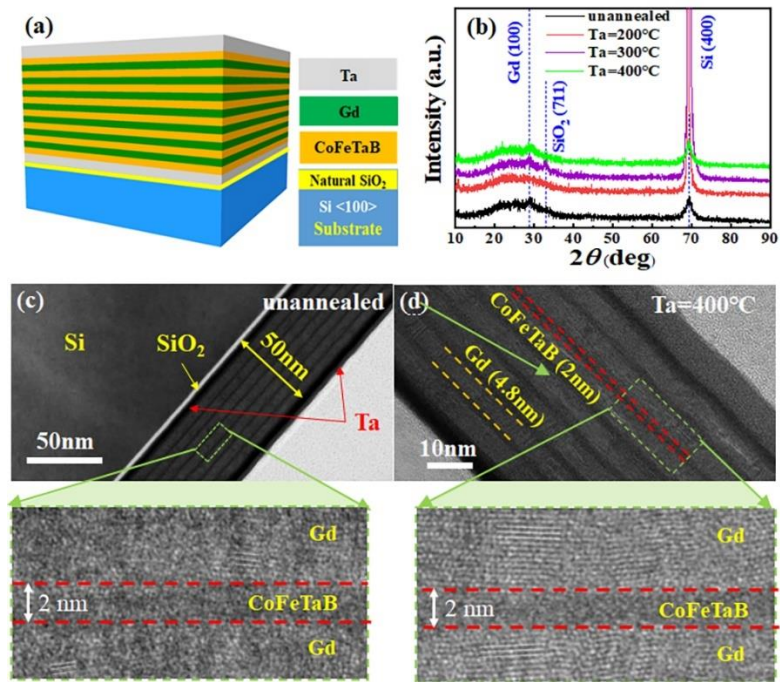


Fig.1. (a) Schematic diagram of multilayer samples and (b) XRD patterns of annealed samples at different temperatures. TEM images of (c) unannealed sample and (d) annealed sample at 400 °C. Insets of (c) and (d) are a partial enlargement.

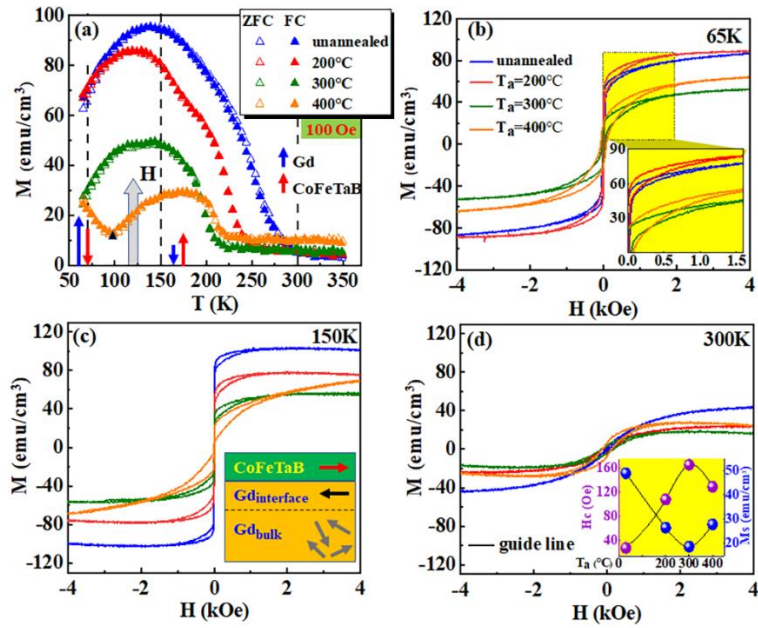


Fig.2. (a) Effect of annealing temperatures on MT characteristics of multilayer structure. The blue \uparrow and red \uparrow in the inset indicate magnetic moments of Gd and CoFeTaB, respectively. Under (b) 65K (inset zooms in on the shaded area), (c) 150K, and (d) 300K, the effect of annealing temperatures on MH characteristics of multilayer structure. Inset of (c) schematically show the $Gd_{interface}$ and Gd_{bulk} regions in Gd layers (arrows are magnetic moment). Inset of (d) show effect of annealing temperatures on M_s and H_c values at 300K.

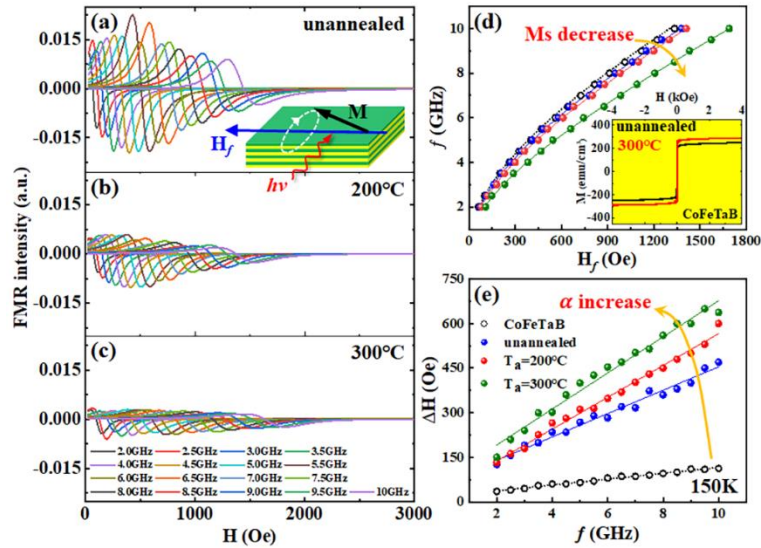


Fig.3. Ferromagnetic resonance spectra of (a) unannealed, (b) 200°C and (c) 300°C annealed multilayer structures. Inset show in-plane FMR schematic diagram. The dependence of (d) H_f and (e) ΔH on FMR frequency of multilayer structures and CoFeTaB films at 150K. Solid and dotted lines represent data fitting lines. Inset of (d) show hysteresis loops for the unannealed and 300°C annealed CoFeTaB films.